

Epimedin C attenuates airway inflammation and remodeling in Asthma by intervening M2 macrophage polarization via modulating the PI3K/Akt/mTOR signaling pathway

Received: 10 November 2025

Accepted: 24 February 2026

Published online: 16 March 2026

Cite this article as: Zhang Z., Cao S., Qin Z. *et al.* Epimedin C attenuates airway inflammation and remodeling in Asthma by intervening M2 macrophage polarization via modulating the PI3K/Akt/mTOR signaling pathway. *Sci Rep* (2026). <https://doi.org/10.1038/s41598-026-42160-4>

Zewen Zhang, Shoubao Cao, Ziwen Qin, Tingting Liu, Qin He, Gen Li, Chuanjun Huang, Yujuan Chen & Yunshan Wang

We are providing an unedited version of this manuscript to give early access to its findings. Before final publication, the manuscript will undergo further editing. Please note there may be errors present which affect the content, and all legal disclaimers apply.

If this paper is publishing under a Transparent Peer Review model then Peer Review reports will publish with the final article.

Epimedin C Attenuates Airway Inflammation and Remodeling in Asthma by intervening M2 macrophage polarization via modulating the PI3K/Akt/mTOR signaling pathway

Zewen Zhang¹, Shoubao Cao², Ziwen Qin³, Tingting Liu⁴, Qin He⁵, Gen Li⁵, Chuanjun Huang⁴, Yujuan Chen^{6*}, Yunshan Wang^{7*}

¹ Department of Radiology, Jinan Central Hospital Affiliated to Shandong First Medical University, 250013, Jinan City, Shandong Province, China

² Department of Internal Medicine, Yangxin County Hospital of Traditional Chinese Medicine, 251800, Yangxin County, Shandong Province, China

³ The First Clinical Medical College, Shandong University of Traditional Chinese Medicine, 250014, Jinan City, Shandong Province, China.

⁴ Department of Respiratory and Critical Care Medicine, Shandong Provincial Hospital Affiliated to Shandong First Medical University, 250021, Jinan City, Shandong Province, China

⁵ Department of Respiratory and Critical Care Medicine, The Traditional Chinese Medicine Hospital of Kashi area, 844000, Kashi City, Xinjiang Uygur Autonomous Region, China.

⁶ Medical College, Shandong University of Traditional Chinese Medicine, 250355, Jinan City, Shandong Province, China

⁷ Medical Experimental Diagnosis Center, Jinan Central Hospital Affiliated to Shandong First Medical University, No. 105 Jiefang Road, Jinan City, Shandong Province, 250013, China

Correspondence to:

Yujuan Chen. Medical College, Shandong University of Traditional Chinese Medicine, 250355, No. 4655, University Road, University Science Park, Changqing District, Jinan City, Shandong Province, China

E-mail: chenyujuan66@163.com

Yunshan Wang: Medical Experimental Diagnosis Center, Jinan Central Hospital Affiliated to Shandong First Medical University, 250013, No. 105 Jiefang Road, Jinan City, Shandong Province,

China.

E-mail: sdjnwys@163.com

ABSTRACT

In bronchial asthma, M2 macrophage polarization and PI3K/Akt/mTOR pathway activation are critically implicated in airway inflammation and remodeling. This study employed an OVA-induced asthmatic mouse model to evaluate the therapeutic effect of Epimedin C, a major flavonoid from *Herba Epimedii* with reported anti-inflammatory and immunoregulatory effects. Pulmonary function tests, histological staining, ELISA, RT-qPCR, and western blotting were utilized to assess airway responsiveness, inflammation, and remodeling. The mechanisms involving the PI3K/Akt/mTOR pathway and macrophage polarization were further investigated via flow cytometry and immunofluorescence. Results showed that Epimedin C significantly improved lung function and alleviated pathological changes. These therapeutic effects were accompanied by suppression of PI3K/Akt/mTOR phosphorylation and inhibition of M2 polarization. Further mechanistic investigation confirmed that M2 polarization was dependent on PI3K/Akt/mTOR activation. Inhibiting this pathway can reverse M2 hyperpolarization and reduce pro-inflammatory mediator production. In conclusion, Epimedin C may alleviate asthma by suppressing M2 macrophage polarization through inhibition of the PI3K/Akt/mTOR pathway. These findings may offer a novel understanding of Epimedin C treatment and furnish evidence for an alternative therapeutic approach to asthma.

Key words: Epimedin C; asthma; airway remodeling; airway inflammation; PI3K/Akt/mTOR signaling pathway □ macrophage polarization; M2 macrophages

Introduction

Bronchial asthma is a heterogeneous inflammatory airway disorder driven by gene-environment interactions, characterized by variable symptoms, airflow obstruction, and airway hyperresponsiveness (AHR) ¹. When exposed to a sensitized environment, the immune response is triggered. Airway inflammation, a crucial component in the pathological mechanism of asthma, releases various inflammatory mediators and cytokines during its process. The repeated or persistent presence of inflammation can impair the airway surface epithelium, promote the epithelial-mesenchymal transition (EMT), and ultimately result in airway remodeling ². A key mechanism in allergic asthma is T helper (Th2)-high airway inflammation, marked by increased expression of Th2 cytokines such as interleukin (IL)-4, IL-5, and IL-13 ³. In recent years, macrophage polarization, the phenotype and specific function transition of macrophage under the stimulation of microenvironment in the body, has been increasingly recognized in asthma pathogenesis. Macrophages manifest two main phenotypes: classically activated macrophages with pro-inflammatory effects (M1) and alternatively activated macrophages with anti-inflammatory effects (M2) ⁴. Th2 cytokines such as IL-4 and IL-13 can induce M2 polarization, releasing anti-inflammatory cytokines such as IL-10 and IL-1, as well as cytokines related to airway inflammation and remodeling such as vascular endothelial growth factor (VEGF) and transforming growth factor (TGF)- β 1, thus exerting a dual role in allergic asthma ⁵. Furthermore, multiple signaling pathways, including JAK/STAT, PI3K/Akt, JNK, and Notch were reported to regulate this process ⁶⁻⁹, offering novel targets for asthma treatment.

Although inhaled corticosteroids (ICS) and bronchodilators are first-line asthma therapies aimed at achieving clinical remission,

patients in remission still exhibit persistent airway inflammation and remodeling compared to healthy individuals^{10,11}. These underlying pathological changes may be detrimental to the maintenance of homeostasis in the remission stage¹², and the efficacy of ICS/long-acting β 2-agonist (LABA) combination therapy in modifying these processes requires further evaluation¹³. Increasing evidence supports the role of traditional Chinese medicine (TCM) in managing both acute asthma attacks and maintaining remission¹⁴. Active components derived from Chinese herbs can alleviate asthma through a multi-target approach, suppressing inflammation, inhibiting airway smooth muscle contraction, and regulating immune balance^{15,16}.

Previous studies have demonstrated that a Chinese herbal compound primarily composed of Epimedium (also known as Herba Epimedii in TCM) mitigated allergic airway inflammation and AHR in asthmatic mice by regulating the PI3K/Akt signaling pathway¹⁷. Additionally, Herba Epimedii and its flavonoids are known to exert anti-inflammatory effects through various pathways, including NF- κ B and MAPK^{18,19}. As a principal and abundant flavonoid glycoside derived from Herba Epimedii²⁰, Epimedin C has shown immunomodulatory potential, as evidenced by its ability to promote lymphocyte proliferation and IL-2 production in an immunosuppressed model²¹. However, the specific pharmacological role of Epimedin C in asthma remains poorly defined. Although macrophage polarization is critical to asthma immunopathology, whether Epimedin C can modulate the allergic immune response by influencing this process is entirely unknown. Furthermore, the potential involvement of the PI3K/Akt/mTOR pathway—a key regulator of macrophage polarization—in mediating its effects has not been investigated.

Therefore, this study aimed to achieve two objectives. First, we sought to determine whether Epimedin C ameliorates airway inflammation and AHR in a murine asthma model. Second, we aimed to provide the first mechanistic evidence that Epimedin C exerts its therapeutic effects by promoting M2 macrophage polarization via the modulation of the PI3K/Akt/mTOR signaling pathway, hoping to offer a new perspective on targeting immune regulation in asthma therapy.

Materials and methods

Reagents and antibodies

Epimedin C ($C_{39}H_{50}O_{19}$, $\geq 98\%$) was purchased from Winherb Medical Technology (Shanghai, China), suspended in 0.5% sodium carboxymethyl cellulose (CMC-Na) at concentrations of 0.002g/ml,

0.004g/ml, 0.008g/ml, and stored at 4°C. The following primary and secondary antibodies were used for western blotting: rabbit antibodies from Cell Signaling Technology (CST; MA, USA) against Vimentin (#5741), α -smooth muscle actin (α -SMA; #19245), Arginase-1(Arg-1; #93668), CD206 (#91992), phosphorylated (p)-PI3K (#17366), p-Akt (#4060), and p-mTOR (#5536); mouse antibodies from CST against PI3K (#13666), Akt (#2920), and mTOR (#4517); and a chicken antibody against β -actin (SAB3500350) from Sigma-Aldrich. Corresponding horseradish peroxidase (HRP) -conjugated secondary antibodies were goat anti-rabbit IgG (GB23204, Servicebio Biology, Wuhan, China), goat anti-mouse IgG (GB23301, Servicebio), and goat anti-chicken IgY (A16054, Thermo Fisher, MA, USA). Antibodies for cell surface and intracellular stain for flow cytometry (F4/80, CD11b, CD86, CD206) were provided by Thermo Fisher. For immunofluorescence, primary antibodies against Arg-1 and CD206 were purchased from CST, while mouse anti-rabbit IgG was obtained from Thermo Fisher.

Cell culture and treatment

Mouse bone marrow-derived macrophages (BMDM) purchased from Procell (CP-M141; Wuhan, China) were cultured in BMDM complete medium (CM-M141; Procell) containing 10% foetal bovine serum (FBS; Hyclone). Culture medium was added with 0.25% trypsin digestion solution (Sigma-Aldrich; Merck KGaA) for passage culture, then placed in a saturated humidified cell culture incubator at 37°C, 5% CO₂ until cell fusion reaches 90%. Cells at 80% confluence were starved for 24h in a culture medium with 1% FBS. The treatment regimens were as follows: after serum starvation, cells were pretreated with or without Epimedin C (100 μ M) for 1 h. Subsequently, IL-4 (10 ng/mL) was added to the cultures, with or without LY294002 (10 μ M), for a 24h stimulation period before harvest. The control group received an equal volume of phosphate-buffered saline (PBS; Servicebio, Wuhan, China) throughout the process. The cytokine concentrations and detection time were obtained based on a pilot study.

Establishment of allergic asthma mouse models

48 healthy BALB/c mice (female, aged 6-8 weeks, weight 18 \pm 2 g) purchased from the Experimental Center of Shandong University (Jinan, China) were housed in a pathogen-free standard environment for 10 days, with a temperature of 20°C, relative humidity of 60%, and a 12-hour (h) light/dark cycle. All mice accepted adaptive feeding for one week before randomly divided into 6 groups, with 8 mice in each group: normal control group (Con), ovalbumins (OVA)-induced asthma group (OVA), low dose of Epimedin C treatment group (Epimedin C-Low, 20mg/kg), middle

dose of Epimedin C treatment group (Epimedin C-Mid, 40mg/kg), high dose of Epimedin C treatment group (Epimedin C-High, 80mg/kg), and dexamethasone treatment group (Dex). Mice from OVA-induced asthma groups were sensitized using 0.2 mL mixed solution containing 100 μ g OVA (Sigma-Aldrich; Merck KGaA, MO, USA) and 2 mg aluminum hydroxide (Sigma-Aldrich; Merck KGaA) by intraperitoneal injection (i.p.) on day 0 and day 7, and challenged with an OVA solution (3% OVA) by atomizing inhalation (i.h.) for 30 minutes (min) daily from day 14 to 28. Reagents for sensitization and challenge in the control group were substituted with PBS. From day 6 to day 7, low, medium, and high doses of Epimedin C were applied once daily by intragastric administration (i.g.) to mice from Epimedin C treatment groups, while mice in the Dex group received 2 mg/kg dexamethasone (Solarbio, Beijing, China) i.p., and distilled water was used on the control group mice. Moreover, 3h before each challenge, from day 14 to day 28, the treatment in each group was the same as described above (Fig. 1A). The lung function was measured 24h after the last challenge, then bronchoalveolar lavage fluid (BALF) and blood were extracted. 6% sodium pentobarbital (Sigma-Aldrich; Merck KGaA) solution prepared with normal saline was administered i.p. to mice at 150 mg/kg for euthanasia. Lung tissues were taken after being sacrificed. All histological quantifications, field selections of stained lung, and functional measurements were performed by an investigator blinded to the group assignments.

Measurement of AHR

Airway responsiveness encompassed indicators of lung resistance (RL) and dynamic lung compliance (C_{dyn}), which were measured by the PFT pulmonary maneuvers system (Buxco Electronics, NY, USA) in an invasive manner. Set the respiratory rate to 90/min and the time of expiration/ inspiration as 20:10. 24h after the last challenge, PBS solution was atomized, and methacholine (Sigma-Aldrich; Merck KGaA, MO, USA) at doses 3.125, 6.25, and 12.5 mg/mL were added sequentially for 8 seconds each time with a 10-min interval. Numerical values were recorded during the intervals, the ratio of which to the baseline (PBS atomization) was conducted as the evaluation index.

Lung tissue staining

After the sacrifice of the mice, the right lungs were extracted and fixed with 10% neutral formalin (Solarbio, Beijing, China) for 5 min. Subsequently, the tissues were embedded in paraffin and sectioned into 5-8 μ m thick slices for subsequent staining. Hematoxylin-Eosin (HE) staining was performed using the HE Stain Kit from Solarbio (Wuhan, China) with hematoxylin and eosin as staining agents.

Periodic Acid Schiff (PAS) staining was performed using 5% periodate alcohol solution, colorless basic fuchsin solution, and hematoxylin as staining agents from the PAS Stain Kit (Solarbio, Beijing, China). Masson staining used magenta staining solution and aniline blue to display collagen deposition in the airways (Masson's Trichrome Stain Kit; Solarbio, Beijing, China). After being dehydrated and sealed, lung tissue staining was utilized to evaluate pathological changes in small and medium airways. We captured images of tangentially intact small and medium airways (with a basement membrane circumference of 100-500 μm) in lung sections from each group, excluding main bronchi and excessively oblique airways. Three eligible airway images were obtained per mouse for assessment. Under optical microscopy, inflammatory infiltration, mucus secretion, and collagen deposition in the eligible airways were observed.

Enzyme-linked immunosorbent assay (ELISA)

After measuring the lung function of mice, 1 ml of PBS was injected into the trachea and washed 3 times to obtain the BALF. Then, the liquid was centrifuged at 4°C and 1200R/min for 5 min to obtain the supernatant, which was preserved in a -80 °C refrigerator. Took the cell culture supernatant with a pipette and centrifuged it at 3000 R/min for 20 min, storing it at -80 °C as above for ELISA. Employed the ELISA kit (Thermo Fisher) to estimate the expression of cytokines in supernatant of BALF and BMDM, following the procedures provided in the product manual.

Western-Blotting (WB) assays

Cells and lung tissues were lysed using radio-immunoprecipitation assay (RIPA) lysis solution (Beyotime, Shanghai, China) containing protease and phosphatase inhibitors. After centrifuging at 4°C, 12000R/m for 10 min, the supernatant, namely the total protein extracts, was obtained, then separated by 10% sodium dodecyl sulfate-polyacrylamide gel electrophoresis (SDS-PAGE) gels and electrotransferred onto polyvinylidene fluoride (PVDF) membranes. To ensure reliable densitometric normalization, the membranes were not cut after transfer; both the internal control β -actin and target proteins were sequentially detected on the same intact membrane. The PVDF membrane was blocked with 5% non-fat milk in tris-buffered saline-tween (TBST; cat. G2150-1L, Servicebio) for 1 h at room temperature (RT) and then incubated overnight at 4°C with primary antibodies. These included rabbit antibodies against Vimentin (1:1000), α -SMA (1:1000), Arg-1 (1:1000), CD206 (1:1000), p-PI3K (1:1000), p-Akt (1:2000), and p-mTOR (1:1000), or mouse antibodies against PI3K (1:1000), Akt (1:2000), and mTOR (1:1000). After incubation, the

membrane was washed 3 times with TBST. It was then incubated with corresponding HRP-conjugated, cross-adsorbed goat anti-rabbit or anti-mouse IgG (1:10000) for 1 h at RT. Protein bands were visualized using enhanced chemiluminescence (ECL). After imaging, the membrane was stripped with Stripping Buffer (cat. 21059, Thermo Fisher) for 15 min at RT and thoroughly washed with TBST 3 times for 10 min each. Complete stripping was confirmed by an ECL check for residual signal. Finally, the membrane was re-probed overnight at 4°C with a chicken monoclonal β -actin antibody (1:8000), followed by an HRP-conjugated anti-chicken IgY secondary antibody (1:10000) and ECL detection. All experiments included at least 3 independent biological replicates. Densitometric analysis was performed using ImageJ software (Version 1.54d; National Institutes of Health, USA; <https://imagej.net/ij/download.html>), and the relative expression levels of each target protein were normalized to the β -actin signal as the loading control.

Reverse transcription-quantitative PCR (RT-qPCR)

Total RNA was extracted from BMDM and mouse lung tissues using TRIzol reagent (Invitrogen, CA, USA). The quantity and concentration of RNA were measured based on absorbance values at A260 nm and A280 nm using the ultraviolet, visible light spectrophotometer (Nd- 1000, Nanodrop, Invitrogen, CA, USA). Utilized the PrimeScript first-strand cDNA synthesis kit (Invitrogen, CA, USA) to reverse transcribe the RNA, the template for reverse transcription, into complementary (c) DNA. Following RT-qPCR was conducted employing SYBR green real-time PCR master mix on an ABI 7000 PCR instrument (Thermo Fisher). The primers: α -SMA, forward 5'-CGGGACATCAAGGAGAACT-3' and reverse 5'-CCCATCAGGCAACTCGTAA-3'; vimentin, forward 5'-TCCACTTTCCGTTCAAGGTC-3' and reverse 5'-AGAGAGAGGAAGCCGAAAGC-3'; CD206, forward 5'-AGGGAAGAGAAGAAGATCCAG-3' and reverse 5'-TGGGAGAAGATGAAGTCAAAC-3'; Arg-1, forward 5'-CTCCAAGCCAAAGTCCTTAGAG-3' and reverse 5'-AGGAGCTGTCATTAGGGACATC-3'; TGF- β 1, forward 5'-ACAATTCTGCGTTACCTT-3' and reverse 5'-GCTAATGTTGTTGCCCTCCTAC-3'; VEGF, forward 5'-TTAGGTAGCATTAGGGGGTCA-3' and reverse 5'-CAGGGATAGGTGGTGGAGATAG-3'. Considering β -actin as the internal parameter, the relative mRNA levels were calculated using the $2^{-\Delta\Delta C_q}$ method. Results were obtained from the average of 8 repeated experiments.

Flow cytometry

Sheared the fresh lung tissues of mice into tiny pieces and ground them into a homogenate in a tissue grinder (Beyotime, Shanghai, China). Followed by centrifuging at 500-800 rpm/min for 2 min to discard the supernatant, rinsing with red blood cell lysis buffer (No. 00-4300-54, Thermo Fisher) to obtain the single-cell suspension. Cells were stained with a fixable viability dye. The single-cell suspension was resuspended in PBS containing a 1:1000 dilution of eFluor 506 Fixable Viability Dye (cat. 65-0866-14, Thermo Fisher), incubated at RT in the dark for 20-30 min, and then washed twice with PBS. Incubated with Fc receptor binding inhibitor (20 μ L/test; No.14-9161-73, Thermo Fisher), then surface stained the cells with F4/80 (0.5 μ g/test; cat.11-4801-82, Thermo Fisher), CD11b (0.125 μ g/test; cat.12-0112-82, Thermo Fisher), CD86 (0.06 μ g/test, cat.17-0862-82, Thermo Fisher) at 4 °C for 30 min. After washing with PBS, fixation buffer (100 μ L/test; No.420801, Thermo Fisher) was used to fix cells at RT in the dark for 40 min before permeabilization with the diluted permeabilization buffer (cat. 00-8333, Thermo Fisher). Stained intracellularly using CD206 antibody (0.125 μ g/test; No.12-2061-82, Thermo Fisher) and incubated at RT in the dark for 30 min. Washed before adding 500 μ L staging buffer to resuspend the cells.

Data Analysis: Data were analyzed using FlowJo software (Version 10.8.1; BD, USA; <https://www.flowjo.com/solutions/flowjo>). A sequential gating strategy was applied: First, cells were gated on FSC-A vs. SSC-A to exclude debris. Singlets were selected using FSC-H vs. FSC-A. Viable cells were identified by negative staining using FVDs (eFluor 506 Fixable Viability Dye) performed before fixation. Macrophages were then defined as F4/80+CD11b+ cells within the live, single-cell population. The frequencies of M1 (CD86+) and M2 (CD206+) subsets were acquired and quantified in parallel within this macrophage gate from the same experiment. Compensation matrices were generated automatically by the FlowJo software using single-stained samples for each fluorochrome and applied to all samples. For each sample, a minimum of 100,000 events in the live cell gate were acquired.

Immunofluorescence

Cells in petri dishes were fixed with 10% neutral formalin (Solarbio, Beijing, China) and permeabilized in 0.1% Triton X-100 (Beyotime, Shanghai, China) for 10 min. After being washed with PBS, antigen retrieval was performed using a heat-induced method with citrate buffer (pH 6.0). The cells were then blocked with 5% bovine serum albumin (BSA) for 1 h at RT. Subsequently, cells were incubated separately overnight at 4°C with rabbit primary antibodies against Arg-1 (1:1000) or CD206 (1:1000), respectively.

Each set of samples was then incubated with an FITC-conjugated goat anti-rabbit IgG (H+L) secondary antibody (1:1000; Thermo Fisher) for 1 h at RT in the dark. After washing with PBS, cell nuclei were counterstained with 4',6-diamidino-2-phenylindole (DAPI; Beyotime, Shanghai, China) for 10 min at RT. Immunofluorescence was observed under a fluorescence microscope (Olympus, Tokyo, Japan). Fluorescence intensities were quantitatively analyzed using ImageJ software.

Statistical analysis

The obtained data were presented as means \pm standard deviation (SD). IBM SPSS Statistics 25 (IBM, USA; <https://www.ibm.com/products/spss-statistics>) was employed to conduct the one-way analysis of variance (ANOVA) for comparing data among multiple groups, followed by Tukey's post hoc test for detailed inter-group comparisons. The pulmonary function data across different methacholine concentration points were analyzed using two-way ANOVA, with treatment group and methacholine concentration as the two independent factors. Pearson correlation coefficient was calculated to assess the relationship between the percentage of M2 macrophages and the phosphorylation levels (p-PI3K/PI3K, p-Akt/Akt, p-mTOR/mTOR) in different groups. A value of $P < 0.05$ was considered to have statistical significance.

Results

Epimedin C suppressed the airway inflammation and remodeling in mice with allergic asthma

To verify the therapeutic effect of Epimedin C on asthma, we initiated with the establishment of the mouse model of OVA-induced allergic asthma. The measurement of the airway responsiveness of mice indicated that RL increased along with the increasing concentrations of methacholine in OVA-treated mice, while Cydn exhibited a trend of gradual decrease (Fig.1 B-C). Furthermore, OVA-induced mice displayed increased Th2 cytokines in BALF (Fig.1 D), notable pathological alterations in lung tissue, such as inflammatory cell infiltration, mucus secretion, and collagen deposition (Fig.2 A-C), as well as elevated expression of emblematic interstitial proteins of EMT, such as vimentin and α -SMA (Fig.3 A, C), compared with the mice in the control group, signifying the successful establishment of the allergic asthma mouse model. Epimedin C treatment can markedly inhibit the increase of RL and impede the decrease of Cydn under the stimulation of each concentration of methacholine on OVA-induced allergic asthma mice, similar to the effect of Dex (Fig.1 B-C), significantly enhancing the lung function of mice. Additionally,

ELISA results demonstrated that the levels of IL-4, IL-5, IL-13, IL-25, and IL-33 were decreased significantly in BALF of mice subjected to the high dose of Epimedin C or Dex treatment (Fig.1 D), along with the reduced protein and mRNA expression of vimentin and α -SMA in lung tissue (Fig.3 A, C), indicating the crucial role of Epimedin C in suppressing airway inflammation and remodeling in asthmatic mice. Lung tissue staining of mice with Epimedin C or Dex treatment revealed reduced infiltration of inflammatory cells around the bronchial and vascular walls, alleviated mucus secretion, mitigated collagen deposition, and tracheal wall and alveolar damage compared to the OVA group (Fig.2 A-C), reflecting the relief of pathological changes in the lung tissues of asthmatic mice by the use of Epimedin C.

To substantiate the dose-dependent effects of Epimedin C, direct comparisons among the dose groups were performed. The results demonstrated that its ameliorative effects on lung function, airway inflammation, and EMT were progressively enhanced with increasing dosage. Specifically, upon methacholine challenge, significant differences in the increase of RL and decrease of Cydn were observed between the low- and mid-dose groups, as well as between the low- and high-dose groups ($P < 0.05$), with the most pronounced difference between the low- and high-dose groups ($P < 0.001$). The levels of inflammatory cytokines in BALF decreased in a stepwise manner with increasing doses. A significant difference in IL-4 level was found between the mid- and high-dose groups ($P < 0.05$), while the levels of IL-5, IL-13, IL-25, and IL-33 showed statistically significant differences between the mid- and high-dose groups, as well as between the low- and high-dose groups ($P < 0.05$ or $P < 0.01$). Furthermore, the protein and mRNA expression levels of Vimentin and α -SMA in lung tissue were significantly reduced in pairwise comparisons among all 3 dose groups (low, mid, and high) ($P < 0.05$) (Tab. s1-2). Collectively, these data confirmed a clear dose-dependent response for Epimedin C in this asthma model.

Epimedin C inhibited the PI3K/Akt/mTOR signaling pathway and M2 macrophage polarization in lung tissues of asthmatic mice

To investigate the underlying mechanisms of Epimedin C in treating asthma inflammation and airway remodeling, we employed WB to detect the PI3K/Akt/mTOR signaling pathway in the lung tissues of mice. WB results displayed that the protein expression of PI3K, Akt, and mTOR was stable between the 6 groups, while the ratio of p-PI3K, p-Akt, p-mTOR to PI3K, Akt, and mTOR in asthmatic mice, namely p-PI3K/PI3K, p-Akt/Akt, p-mTOR/TOR, was significantly elevated compared to the control group, indicating

that the activated PI3K/Akt/mTOR signaling pathway is involved in the pathogenesis of asthma. Furthermore, the treatment of Epimedin C or Dex led to a reduction in p-PI3K/PI3K, p-Akt/Akt, and p-mTOR/mTOR, with the higher dose of Epimedin C causing a more significant ratio decrease. These ratios among 3 dose groups (low, mid, and high) all showed statistically significant differences ($P < 0.01$) (Tab. s3). 40g/kg (high dose) Epimedin C exerted a similar inhibitory effect on the pathway as Dex, suggesting that Epimedin C might improve asthma inflammation and airway remodeling by inhibiting the activation of the PI3K/Akt/mTOR pathway (Fig.4 A). Considering that the PI3K/Akt signaling pathway is known to be closely related to the polarization of macrophages towards the M2 subtype, we detected the expression of M2 macrophage markers Arg-1 and CD206 using WB and RT-qPCR. The result showed that the expression of Arg-1 and CD206 in lung tissue of asthmatic mice was obviously increased compared to the control group, and this high expression can be significantly inhibited by high-dose Epimedin C or Dex, implying the regulatory effect of Epimedin C on M2 macrophage polarization (Fig.3 B, D). In addition, flow cytometry was applied to sort M2 macrophages in lung tissue homogenate (Fig.4 B), finding that the percentage trend of M2 macrophages between groups was positively correlated with the trend of p-PI3K/PI3K, p-Akt/Akt, and p-mTOR/mTOR detected by WB (Fig.4 C, $0 < r < 1$, $p < 0.05$). Therefore, we speculated that Epimedin C may restrain M2 macrophage polarization by inhibiting the activation of the PI3K/Akt pathway, thereby exerting a therapeutic effect on asthma.

Down-regulation of the PI3K/Akt/mTOR signaling pathway can inhibit the M2 macrophage polarization

To explore whether the PI3K/Akt/mTOR signaling pathway can intervene in M2 macrophage polarization in asthma, we cultured BMDM cells and induced them using IL-4 to differentiate into M2 macrophages. Immunofluorescence and RT-qPCR results displayed that BMDM cells induced by IL-4 exhibited high expression of M2 biomarkers Arg-1 and CD206 (Fig.5 A-C). In addition, RT-qPCR and ELISA revealed increased VEGF and TGF- β 1 secreted by M2 macrophages (Fig.5 D, E), indicating that IL-4 successfully induced macrophage polarization towards the M2 subtype. WB was employed to detect the cells, finding that the IL-4 group showed elevated p-PI3K/PI3K, p-Akt/Akt, and p-mTOR/mTOR (Fig.6), indicating that the induction of M2 macrophages by IL-4 entails the activation of the PI3K/Akt signaling pathway. After adding PI3K/Akt/mTOR pathway inhibitor LY294002 on the basis of IL-4 induction, Arg-1, CD206, VEGF, and TGF- β 1 were detected to have

a significant decrease in expression (Fig.5), implying that the polarization process of M2 macrophages requires the involvement of the activated PI3K/Akt/mTOR signaling pathways. Therefore, down-regulating the PI3K/Akt/mTOR signaling pathway may be a practical approach to inhibit the hyperpolarization of M2 macrophages.

Epimedin C inhibited M2 macrophage polarization through down-regulation of the PI3K/Akt/mTOR signaling pathway to improve airway inflammation and remodeling in asthma

In vivo experiments have discovered that Epimedin C can improve airway inflammation and remodeling in asthma by inhibiting the PI3K/Akt/mTOR signaling pathway, while IL-4-induced polarization of M2 macrophages in DMBMs can be reversed by inhibiting the pathway. Furthermore, treatment of IL-4-induced BMDMs with Epimedin C significantly reduced the expression of M2 markers Arg-1 and CD206, demonstrating an inhibitory effect comparable to that of the specific PI3K/Akt inhibitor LY294002 (Fig.5 A-C). The WB results revealed that p-PI3K/PI3K, p-Akt/Akt, and p-mTOR/mTOR in BMDM cells of the IL-4+Epimedin C group were obviously reduced, confirmed that Epimedin C potently inhibited the activation of the PI3K/Akt/mTOR pathway (Fig.6). Notably, the combination of Epimedin C with LY294002 did not produce a significantly greater inhibitory effect than Epimedin C alone ($p > 0.05$), suggesting that Epimedin C's action may converge on the PI3K/Akt/mTOR pathway to attenuate M2 macrophage differentiation. The expression levels of VEGF and TGF- β 1 in cells or cell supernatants were assessed using RT-qPCR and ELISA, respectively. The results showed that using Epimedin C on IL-4-incubated BMDM can significantly reduce the secretion of pro-inflammatory and pro-EMT proteins VEGF and TGF- β 1 secreted by M2 macrophages, which had a comparable effect to LY294002 (Fig5 D, E), indicating that Epimedin C may inhibit M2 macrophage polarization by down-regulating the PI3K/Akt/mTOR signaling pathway, thereby alleviated airway inflammation and remodeling in asthma.

Discussion

Asthma exhibits heterogeneity in symptoms and pathological mechanisms, with chronic airway inflammation and remodeling as the main pathological changes. Although glucocorticoids (GCs) are first-line therapies, their limitations necessitate the search for alternative treatments. Flavonoids derived from Epimedium have demonstrated anti-inflammatory properties¹⁸. For instance, Icariin alleviates asthma inflammation in both in vivo and in vitro models

²², Epimedin C has been shown to improve asthma inflammation and AHR, as well ²³. However, the specific mechanisms of Epimedin C in suppressing asthmatic inflammation remain unclear.

In this study, we used an OVA-induced murine model of allergic asthma to evaluate Epimedin C administered orally. Epimedin C treatment significantly ameliorated AHR and reversed the characteristic elevation of Th2 cytokines in BALF. The over-expression of α -SMA and vimentin, which indicate the airway inflammation and EMT in asthma, was also markedly reduced. Furthermore, Epimedin C alleviated pathological lung changes, including inflammatory infiltration, airway wall thickening, collagen deposition, and mucus hypersecretion. Collectively, these findings demonstrated that Epimedin C effectively attenuated airway inflammation and remodeling in a dose-dependent manner, with the high-dose effect being comparable to that of Dex.

Our previous studies found that a TCM formula mainly consisting of Epimedium can treat asthma through multiple targets and pathways; the therapeutic effects mainly involve the PI3K/Akt/mTOR signaling pathway ¹⁷. A study of network pharmacology and molecular docking found that the active constituents of Epimedium Folium, including Epimedin C, can exert a protective effect on cisplatin-induced intestinal injury by regulating PI3K-Akt, caspase, and NF- κ B signaling pathways ²⁴. Another network pharmacology and metabolomics analysis of Epimedium against liver cancer also reported that the PI3K/Akt signaling pathway and arachidonic acid metabolism may be associated with Epimedium's efficacy ²⁵. Moreover, as Epimedin C is considered the main flavonoid glycoside derived from Epimedium, we hypothesized that the PI3K/Akt/mTOR signaling pathway might be a crucial target for Epimedin C to exert anti-inflammatory and anti-remodeling effects in asthma. Previous studies have demonstrated that the PI3K/Akt signaling pathway can regulate the inflammatory response in asthma airways via various downstream signaling molecules²⁶. Blocking the PI3K/Akt signaling pathway could reduce the infiltration of inflammatory cells in lung tissue, thereby inhibiting airway inflammation and goblet cell proliferation-induced mucus hypersecretion ²⁷. On the other hand, the activation of the PI3K/Akt signaling pathway may stimulate the activation of eosinophils, facilitate the formation and angiogenesis of fibroblasts, lead to the proliferation of airway smooth muscle cells, vasodilation, and luminal stenosis, thereby causing airway remodeling ²⁸. As an effector protein downstream of Akt, the upstream subtype of mTOR, mTOR1, can activate Akt, while the downstream mTOR2 can participate in cell growth and apoptosis

through autophagy²⁹. Inhibiting the phosphorylation of PI3K, Akt, and mTOR can suppress the airway epithelial autophagy to alleviate airway inflammation, remodeling, and oxidative stress in asthma³⁰. In summary, our mechanistic focus on the PI3K/Akt/mTOR axis was predicated on prior evidence from compound formulations, network pharmacology predictions, and its established central role in asthma. The consistent inhibition of this pathway and the concomitant functional improvements by Epimedin C in both in vivo and in vitro models validated our initial hypothesis and the rationale for this focused investigation.

In our study, WB was used to detect the PI3K/Akt/mTOR signaling pathway in the lung tissues of mice, discovering that the pathway was activated in asthmatic mice, which is consistent with previous reports. Moreover, we found that Epimedin C can significantly down-regulate the phosphorylation levels of PI3K, Akt, and mTOR, inhibiting the activation of the pathway, thus suppressing airway inflammation and slowing down the progression of EMT, exerting an important therapeutic role in asthma.

Subsequently, we turned our attention to exploring how the inhibited PI3K/Akt/mTOR pathway suppresses inflammation in asthma. It is known that the activated PI3K/Akt signaling pathway can induce helper T cells to differentiate into Th2 cells, secreting inflammatory cytokines such as IL-4, IL-5, and TNF- α . IL-4 not only participates in allergic inflammation and airway remodeling in asthma, but also induces macrophage polarization into M2 macrophages³¹. Over-polarization of M2 macrophages leads to eosinophilic infiltration in the airways, mainly involving mediators of IL-4, IL-5, IL-9, and IL-13. This promotes the migration and infiltration of eosinophils and mast cells into the lungs, influencing vascular permeability, smooth muscle contraction, cell recruitment, mucus production, and goblet cell secretion, further exacerbating the severity of asthma³². To verify the involvement of M2 macrophages in the pathological process of asthma, we detected the biomarker proteins of M2 macrophages, such as Arg-1 and CD206, in the lung tissue of asthmatic mice, and performed flow cytometry sorting on M2 macrophages. Results showed that M2 macrophages in asthmatic mice were highly expressed, and M2 macrophage markers were reduced after Epimedin C treatment. The inter-group changes were positively correlated with phosphorylated PI3K, Akt, and mTOR, indicating that the activation of the PI3K/Akt/mTOR pathway is closely related to M2 macrophage polarization, while Epimedin C may exert therapeutic effects on asthma by regulating this process.

Finally, to directly validate whether macrophages are the key cellular target through which Epimedin C exerts its anti-asthmatic effects *in vivo*, we conducted complementary *in vitro* experiments using IL-4-induced BMDMs. The *in vivo* data demonstrated that Epimedin C administration reduced M2 macrophage markers in lung tissue and concurrently inhibited the PI3K/Akt/mTOR pathway. To establish a causal link, we examined whether Epimedin C could directly inhibit IL-4-induced M2 polarization of BMDMs via the same pathway. Consistent with the *in vivo* findings, Epimedin C treatment significantly suppressed the expression of M2 markers (Arg-1, CD206) and the secretion of related factors (VEGF, TGF- β 1) in BMDMs, which was associated with the inhibition of PI3K/Akt/mTOR activation. This concordance between the *in vivo* and *in vitro* systems strongly suggested that the amelioration of asthma by Epimedin C was, at least in part, mediated through its direct action on macrophages to attenuate their PI3K/Akt/mTOR-driven M2 polarization. Arg-1 released by M2 macrophages can induce eosinophil aggregation towards inflammatory sites, participating in the formation of asthma airway remodeling³³. Being a cytokine secreted by M2 macrophages, VEGF is considered an important mediator of vascular remodeling and inflammation in asthma, which enhances allergic reactions³⁴. In addition, TGF- β 1 is also a key factor secreted by M2 macrophages that can participate in EMT by mediating the PI3K/Akt pathway³⁵. Therefore, hyperpolarized M2 macrophages in allergic asthma can promote airway inflammation and remodeling through highly secreted Arg-1, VEGF, and TGF- β 1, consistent with the previous report, which suggested that macrophages stimulated by IL-4 had an augmented immune response to subsequent stimulation by altering cellular metabolism and epigenetic modifications, exhibiting significantly enhanced pro-inflammatory capacity³⁶.

On this basis, the PI3K/Akt pathway inhibitor LY294002 was used to inhibit the phosphorylation of PI3K, Akt, and mTOR, leading to significant decreases in Arg-1, CD206, VEGF, and TGF- β 1, indicating that suppressing the PI3K/Akt/mTOR pathway can effectively inhibit M2 macrophage polarization to down-regulate the expression of pro-inflammatory cytokines secreted by M2 macrophages. To verify the targeted therapeutic effect of Epimedin C on M2 macrophage polarization, we applied Epimedin C to BMDMs incubated with IL-4. The cells also showed reduced levels of phosphorylated PI3K, Akt, and mTOR, as well as Arg-1, CD206, VEGF, and TGF- β 1, which were similar or even lower in expression compared to the cells in the IL-4 \square LY294002 group. In brief, the

above evidence supported our conclusion that Epimedin C may inhibit M2 macrophage polarization via inhibiting the activation of the PI3K/Akt/mTOR signaling pathway to alleviate airway inflammation and remodeling in asthma.

While this study provided the mechanistic insight of Epimedin C ameliorating asthma, certain limitations should be noted.

First, systematic pharmacokinetic studies (e.g., oral bioavailability) of the pure Epimedin C monomer in mice are currently lacking, which somewhat limits more precise dose optimization. Although the dose-dependent therapeutic effects observed across multiple dose groups supported the regimen's validity, the pharmacokinetic properties of Epimedin C remain to be elucidated. On the other hand, as a proof-of-concept investigation, systematic toxicological evaluations of Epimedin C were not performed. Although no overt signs of toxicity were observed during the treatment, literature on related compounds supports its tolerability; a definitive toxicity profile warrants comprehensive assessment in future preclinical development. Addressing these aspects will be crucial for advancing Epimedin C toward a potential therapeutic agent.

Second, a limitation of this study is its focused investigation on the PI3K/Akt/mTOR pathway. As a multi-target flavonoid, Epimedin C may engage other immunomodulatory pathways known to be relevant in asthma, such as NF- κ B or MAPK. Our current data did not exclude potential contributions from these "off-target" effects to the overall therapeutic outcome. Future studies employing techniques like phospho-protein arrays or RNA sequencing could more comprehensively map the signaling landscape modulated by Epimedin C, helping to distinguish its primary mechanism from secondary or synergistic effects.

Moreover, while we have demonstrated both *in vivo* and *in vitro* that Epimedin C inhibited the PI3K/Akt/mTOR pathway and reduced M2 macrophages, the lack of macrophage-specific depletion or lineage-tracing experiments prevented us from entirely ruling out its potential direct effects on other pivotal cell types in asthma, such as epithelial cells or fibroblasts. Therefore, the conception that macrophages serve as the primary cellular target requires further validation. Future studies employing cell-specific knockout models would be valuable to substantiate the central mediating role of macrophages and to elucidate the integrated modulatory effects of Epimedin C within the complex cellular network of asthma.

Conclusion

To summarize, this article aimed to explore the intrinsic mechanisms of Epimedin C in the treatment of bronchial asthma. We found that Epimedin C could suppress the activation of the PI3K/Akt/mTOR signaling pathways, thereby inhibiting the polarization of macrophages towards M2, and reducing the expression of inflammation and airway remodeling-related factors secreted by M2 macrophages. This mechanism was speculated to regulate airway inflammation and remodeling in asthma, acting as an essential process during Epimedin C, exerting its therapeutic effects. The findings thus provided a scientific rationale for Epimedin C's development as a potential compound against asthma, offering a novel perspective for applying TCM in treating inflammatory respiratory diseases.

Funding

This study was supported by the National Nature Science Foundation of China grant (No. 82405322) and the Natural Science Foundation of Shandong Province Youth Program of China (No. ZR2023QH089).

Author contributions statement

ZZ, YC, and YW conceived and designed the review. ZZ, SC, and ZQ wrote the manuscript and prepared the figures. TL, YW, and YC performed the literature search. YC, ZZ, CH, and YW revised it critically for important intellectual content. All authors have read and approved the final manuscript. All authors are responsible for all aspects of the work and approve the submission in its current form. Data authentication is not applicable.

Availability of data and materials

The datasets during and/or analyzed during the current study are available from the corresponding author upon reasonable request.

Ethics approval

The animal studies were approved by the ethics committee on animal care of Shandong Provincial Hospital & Shandong First Medical University, Jinan, China (2024-553). All experiments meet the requirements of the ARRIVE guidelines. All animal studies were carried out in accordance with the NIH guidelines in 2011 for the care and use of laboratory animals.

Competing Interest

The authors declare no conflict of interest.

Figure legends:

Figure 1. Establishment and verification of the allergic asthma mouse model.

(A) Protocol of OVA-induced allergic asthma and treatment; (B) Airway responsiveness measured by C_{dyn} in response to methacholine; (C) Airway responsiveness measured by RL in response to methacholine; (D) Inflammatory cytokines in BALF detected by ELISA, including IL-4, IL-5, IL-13, IL-25, and IL-33.

n=8 for A~D. *P<0.05, **P<0.01, ***P<0.001, and ****P<0.0001 compared to control group. #P<0.05, ##P<0.01, ###P<0.001, and ####P<0.0001 compared to the OVA group. &P<0.05 Epimedin C-High group compared to the DEX group. RL, lung resistance; C_{dyn}, dynamic lung compliance; IL, interleukin; BALF, bronchoalveolar lavage fluid; Dex, dexamethasone; OVA, ovalbumin; PBS, phosphate-buffered saline; alum, aluminum hydroxide; DW, distilled water; i.p., intraperitoneal injection; i.g., intragastric administration; i.h., atomizing inhalation.

Figure 2. Epimedin C alleviated pathological changes in the lung tissue of asthmatic mice.

Representative images of tangentially intact small and medium airways (with a basement membrane circumference of 100-500 μm) in lung sections from each mouse group. Scale bar: 25 μm. (A) HE staining; (B) PAS staining; (C) Masson staining. HE, hematoxylin and eosin; PAS, periodic acid-schiff; Dex, dexamethasone.

Figure 3. Epimedin C reduced the expression of M2 macrophage biomarkers of inflammation and EMT in asthma.

(A) WB detected the protein of α-SMA and vimentin in lung tissues; (B) WB detected the protein of Arg-1 and CD206 in lung tissues; (C) RT-qPCR detected the mRNA levels of α-SMA and vimentin in lung tissues; (D) RT-qPCR detected the mRNA levels of Arg-1 and CD206 in lung tissues.

n=3 for A,B; n=8 for C,D. *P<0.05, **P<0.01, ***P<0.001, and ****P<0.0001 compared to control group. #P<0.05, ##P<0.01, ###P<0.001, and ####P<0.0001 compared to the OVA group. &P<0.05, &&P<0.01, and &&&P<0.001 compared the Epimedin C-high group to the Dex group. Dex, dexamethasone; Arg-1, Arginase-1; L, low; M, middle; H, high.

Figure 4. Epimedin C down-regulated the PI3K/Akt/mTOR

signaling pathways and M2 macrophage polarization in vivo.

(A) WB detected the proteins of p-PI3K, PI3K, p-Akt, Akt, p-mTOR, and mTOR in lung tissues; (B) flow cytometry sorted M1/M2 macrophages in lung tissues; (C) The correlation of the trend of M2 macrophages (%) and the trend of p-PI3K/PI3K, p-Akt/Akt, and p-mTOR/mTOR (%) between 6 groups. $n=3$ for A, B. $*P<0.05$, $**P<0.01$, $***P<0.001$, and $****P<0.0001$ compared to control group. $\#P<0.05$, $\#\#P<0.01$, $\#\#\#P<0.001$, and $\#\#\#\#P<0.0001$ compared to OVA group, $\&\&\&P<0.001$ Epimedin C-High group compared to the DEX group. p-, phosphorylated; PI3K, Phosphatidylinositol-3-kinase; Akt, Protein kinase B; mTOR, mammalian target of rapamycin; Dex, dexamethasone.

Figure 5. Epimedin C inhibited M2 macrophage markers, pro-inflammatory, and pro-EMT factors in vitro.

(A) Immunofluorescence detected Arg-1 in BMDMs; (B) Immunofluorescence detected CD206 in BMDMs; (C) RT-qPCR detected mRNA relative expression of Arg-1 and CD206; (D) RT-qPCR detected mRNA relative expression of VEGF and TGF- β 1; (E) ELISA detected VEGF and TGF- β 1 in the BMDMs supernatant. $n=8$ for A~E. $*P<0.05$, $**P<0.01$, $***P<0.001$, and $****P<0.0001$ compared to control group. $\#\#\#P<0.001$ and $\#\#\#\#P<0.0001$ compared to the IL-4 group. $\&P<0.05$, $\&\&P<0.01$, and $\&\&\&P<0.001$ compared between annotated groups. Arg-1, Arginase-1; VEGF, vascular endothelial growth factor; TGF- β 1, transforming growth factor- β 1; BMDM, bone marrow-derived macrophage.

Figure 6. Epimedin C down-regulated the PI3K/Akt/mTOR signaling pathway in vitro.

$n=3$. $*P<0.05$, $***P<0.001$, and $****P<0.0001$ compared to control group. $\#\#\#P<0.001$ and $\#\#\#\#P<0.0001$ compared to the IL-4 group. $\&\&\&P<0.001$ and $\&\&\&\&P<0.0001$ compared to the IL-4 \square LY294002 group. p-, phosphorylated; IL, interleukin; PI3K, phosphatidylinositol-3-kinase; Akt, protein kinase B; mTOR, mammalian target of rapamycin.

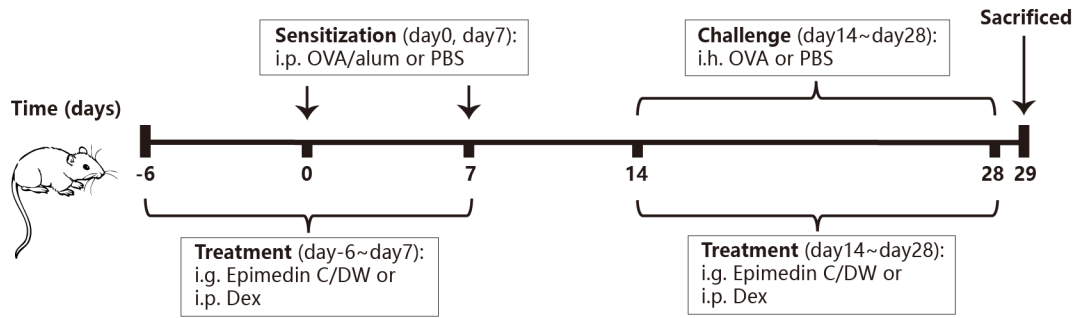
References

- 1 Venkatesan, P. 2023 GINA report for asthma. *Lancet Respir Med* **11**, 589, doi:10.1016/s2213-2600(23)00230-8 (2023).
- 2 Papi, A., Brightling, C., Pedersen, S. E. & Reddel, H. K. Asthma. *Lancet* **391**, 783-800, doi:10.1016/s0140-6736(17)33311-1 (2018).
- 3 Fahy, J. V. Type 2 inflammation in asthma--present in most, absent in many. *Nat Rev Immunol* **15**, 57-65, doi:10.1038/nri3786 (2015).
- 4 Liu, Y. C., Zou, X. B., Chai, Y. F. & Yao, Y. M. Macrophage polarization in inflammatory diseases. *Int J Biol Sci* **10**, 520-529, doi:10.7150/ijbs.8879 (2014).
- 5 Abdelaziz, M. H. *et al.* Alternatively activated macrophages; a double-edged sword in allergic asthma. *J Transl Med* **18**, 58, doi:10.1186/s12967-020-02251-w (2020).
- 6 Cui, Y. *et al.* TREM2 deficiency aggravates renal injury by promoting macrophage apoptosis and polarization via the JAK-STAT pathway in mice. *Cell Death Dis* **15**, 401, doi:10.1038/s41419-024-06756-w (2024).
- 7 Feng, H., Zhang, D., Yin, Y., Kang, J. & Zheng, R. Salidroside ameliorated the pulmonary inflammation induced by cigarette smoke via mitigating M1 macrophage polarization by JNK/c-Jun. *Phytother Res* **37**, 4251-4264, doi:10.1002/ptr.7905 (2023).
- 8 Liu, Z. *et al.* Activated Notch1 promotes macrophage polarization and exacerbates sepsis-induced acute lung injury via β -catenin/NF- κ B signaling. *Biochem Pharmacol* **236**, 116892, doi:10.1016/j.bcp.2025.116892 (2025).
- 9 Qiao, X. *et al.* Grape Seed Proanthocyanidin Ameliorates LPS-induced Acute Lung Injury By Modulating M2a Macrophage Polarization Via the TREM2/PI3K/Akt Pathway. *Inflammation* **46**, 2147-2164, doi:10.1007/s10753-023-01868-5 (2023).
- 10 Boulet, L. P., Turcotte, H. & Brochu, A. Persistence of airway obstruction and hyperresponsiveness in subjects with asthma remission. *Chest* **105**, 1024-1031, doi:10.1378/chest.105.4.1024 (1994).
- 11 Carpaij, O. A., Burgess, J. K., Kerstjens, H. A. M., Nawijn, M. C. & van den Berge, M. A review on the pathophysiology of asthma remission. *Pharmacol Ther* **201**, 8-24, doi:10.1016/j.pharmthera.2019.05.002 (2019).
- 12 van den Toorn, L. M. *et al.* Airway inflammation is present during clinical remission of atopic asthma. *Am J Respir Crit Care Med* **164**, 2107-2113, doi:10.1164/ajrccm.164.11.2006165 (2001).
- 13 Kim, L. H. Y., Saleh, C., Whalen-Browne, A., O'Byrne, P. M. & Chu, D. K. Triple vs Dual Inhaler Therapy and Asthma Outcomes in Moderate to Severe Asthma: A Systematic Review and Meta-analysis. *Jama* **325**, 2466-2479, doi:10.1001/jama.2021.7872 (2021).
- 14 Liao, P. F., Wang, Y. T., Wang, Y. H., Chiou, J. Y. & Wei, J. C. C. Traditional Chinese medicine use may reduce medical utility in patients with asthma:

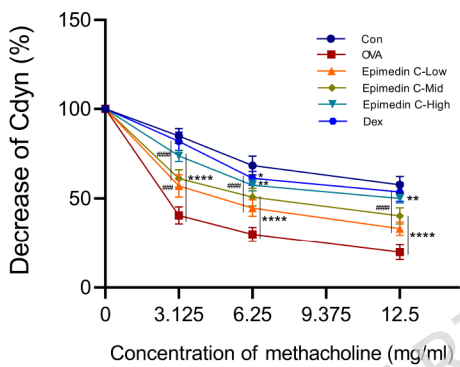
- a nationwide population-based retrospective cohort study. *Qjm* **114**, 857-864, doi:10.1093/qjmed/hcaa252 (2022).
- 15 Li, X. M. & Brown, L. Efficacy and mechanisms of action of traditional Chinese medicines for treating asthma and allergy. *J Allergy Clin Immunol* **123**, 297-306; quiz 307-298, doi:10.1016/j.jaci.2008.12.026 (2009).
- 16 Wang, W. *et al.* Active ingredients from Chinese medicine plants as therapeutic strategies for asthma: Overview and challenges. *Biomed Pharmacother* **137**, 111383, doi:10.1016/j.biopha.2021.111383 (2021).
- 17 Qin, Z. *et al.* Mechanisms of Bushenyiqi decoction in the treatment of asthma: an investigation based on network pharmacology with experimental validation. *Front Pharmacol* **15**, 1361379, doi:10.3389/fphar.2024.1361379 (2024).
- 18 Oh, Y. C. *et al.* Inhibitory Effects of Epimedium Herb on the Inflammatory Response In Vitro and In Vivo. *Am J Chin Med* **43**, 953-968, doi:10.1142/s0192415x1550055x (2015).
- 19 Yin, L. L., Lin, L. L., Zhang, L. & Li, L. Epimedium flavonoids ameliorate experimental autoimmune encephalomyelitis in rats by modulating neuroinflammatory and neurotrophic responses. *Neuropharmacology* **63**, 851-862, doi:10.1016/j.neuropharm.2012.06.025 (2012).
- 20 Zhang, H. *et al.* Comparison of the Active Compositions between Raw and Processed Epimedium from Different Species. *Molecules* **23**, doi:10.3390/molecules23071656 (2018).
- 21 Liang, H. R., Vuorela, P., Vuorela, H. & Hiltunen, R. Isolation and immunomodulatory effect of flavonol glycosides from Epimedium hunanense. *Planta Med* **63**, 316-319, doi:10.1055/s-2006-957690 (1997).
- 22 Liu, J. *et al.* Icaritin Protects Hippocampal Neurons From Endoplasmic Reticulum Stress and NF- κ B Mediated Apoptosis in Fetal Rat Hippocampal Neurons and Asthma Rats. *Front Pharmacol* **10**, 1660, doi:10.3389/fphar.2019.01660 (2019).
- 23 Huang, M., Wei, Y. & Dong, J. Epimedin C modulates the balance between Th9 cells and Treg cells through negative regulation of noncanonical NF- κ B pathway and MAPKs activation to inhibit airway inflammation in the ovalbumin-induced murine asthma model. *Pulm Pharmacol Ther* **65**, 102005, doi:10.1016/j.pupt.2021.102005 (2020).
- 24 Xia, J. *et al.* Based on network pharmacology and molecular docking to explore the protective effect of Epimedii Folium extract on cisplatin-induced intestinal injury in mice. *Front Pharmacol* **13**, 1040504, doi:10.3389/fphar.2022.1040504 (2022).
- 25 Liu, Y. M. *et al.* Uncovering the key pharmacodynamic material basis and possible molecular mechanism of extract of Epimedium against liver cancer through a comprehensive investigation. *J Ethnopharmacol* **317**, 116765, doi:10.1016/j.jep.2023.116765 (2023).
- 26 Ma, B., Athari, S. S., Mehrabi Nasab, E. & Zhao, L. PI3K/AKT/mTOR and TLR4/MyD88/NF- κ B Signaling Inhibitors Attenuate Pathological Mechanisms

- of Allergic Asthma. *Inflammation* **44**, 1895-1907, doi:10.1007/s10753-021-01466-3 (2021).
- 27 Peng, W. *et al.* FGF10 attenuates allergic airway inflammation in asthma by inhibiting PI3K/AKT/NF- κ B pathway. *Cell Signal* **113**, 110964, doi:10.1016/j.cellsig.2023.110964 (2024).
- 28 Liu, Y. *et al.* Emodin ameliorates ovalbumin-induced airway remodeling in mice by suppressing airway smooth muscle cells proliferation. *Int Immunopharmacol* **88**, 106855, doi:10.1016/j.intimp.2020.106855 (2020).
- 29 Zhang, Y. *et al.* Activation of the mTOR signaling pathway is required for asthma onset. *Sci Rep* **7**, 4532, doi:10.1038/s41598-017-04826-y (2017).
- 30 Nguyen, V. *et al.* Zi-Su-Zi decoction improves airway hyperresponsiveness in cough-variant asthma rat model through PI3K/AKT1/mTOR, JAK2/STAT3 and HIF-1 α /NF- κ B signaling pathways. *J Ethnopharmacol* **314**, 116637, doi:10.1016/j.jep.2023.116637 (2023).
- 31 García-Fojeda, B., Minutti, C. M., Montero-Fernández, C., Stämme, C. & Casals, C. Signaling Pathways That Mediate Alveolar Macrophage Activation by Surfactant Protein A and IL-4. *Front Immunol* **13**, 860262, doi:10.3389/fimmu.2022.860262 (2022).
- 32 Dasgupta, P. *et al.* The adaptor protein insulin receptor substrate 2 inhibits alternative macrophage activation and allergic lung inflammation. *Sci Signal* **9**, ra63, doi:10.1126/scisignal.aad6724 (2016).
- 33 Nguyen, J. *et al.* Immunophenotyping of Acute Inflammatory Exacerbations of Lung Injury Driven by Mutant Surfactant Protein-C: A Role for Inflammatory Eosinophils. *Front Pharmacol* **13**, 875887, doi:10.3389/fphar.2022.875887 (2022).
- 34 Tota, M., Łacwik, J., Laska, J., Sędek, Ł. & Gomułka, K. The Role of Eosinophil-Derived Neurotoxin and Vascular Endothelial Growth Factor in the Pathogenesis of Eosinophilic Asthma. *Cells* **12**, doi:10.3390/cells12091326 (2023).
- 35 Riemma, M. A. *et al.* Sphingosine-1-phosphate/TGF- β axis drives epithelial mesenchymal transition in asthma-like disease. *Br J Pharmacol* **179**, 1753-1768, doi:10.1111/bph.15754 (2022).
- 36 Dang, B. *et al.* The glycolysis/HIF-1 α axis defines the inflammatory role of IL-4-primed macrophages. *Cell Rep* **42**, 112471, doi:10.1016/j.celrep.2023.112471 (2023).

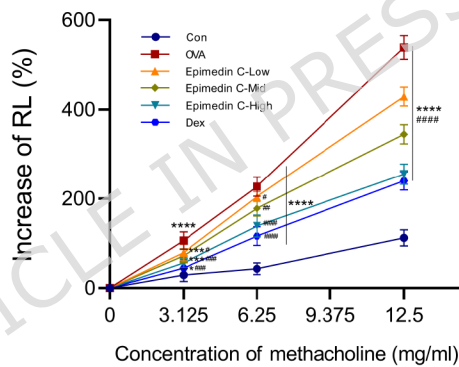
(A)



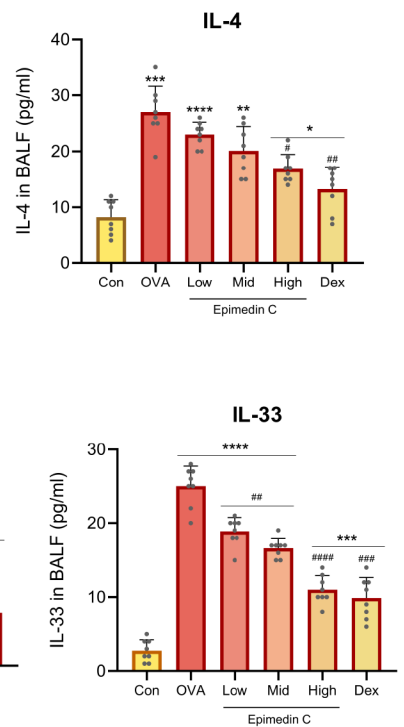
(B)

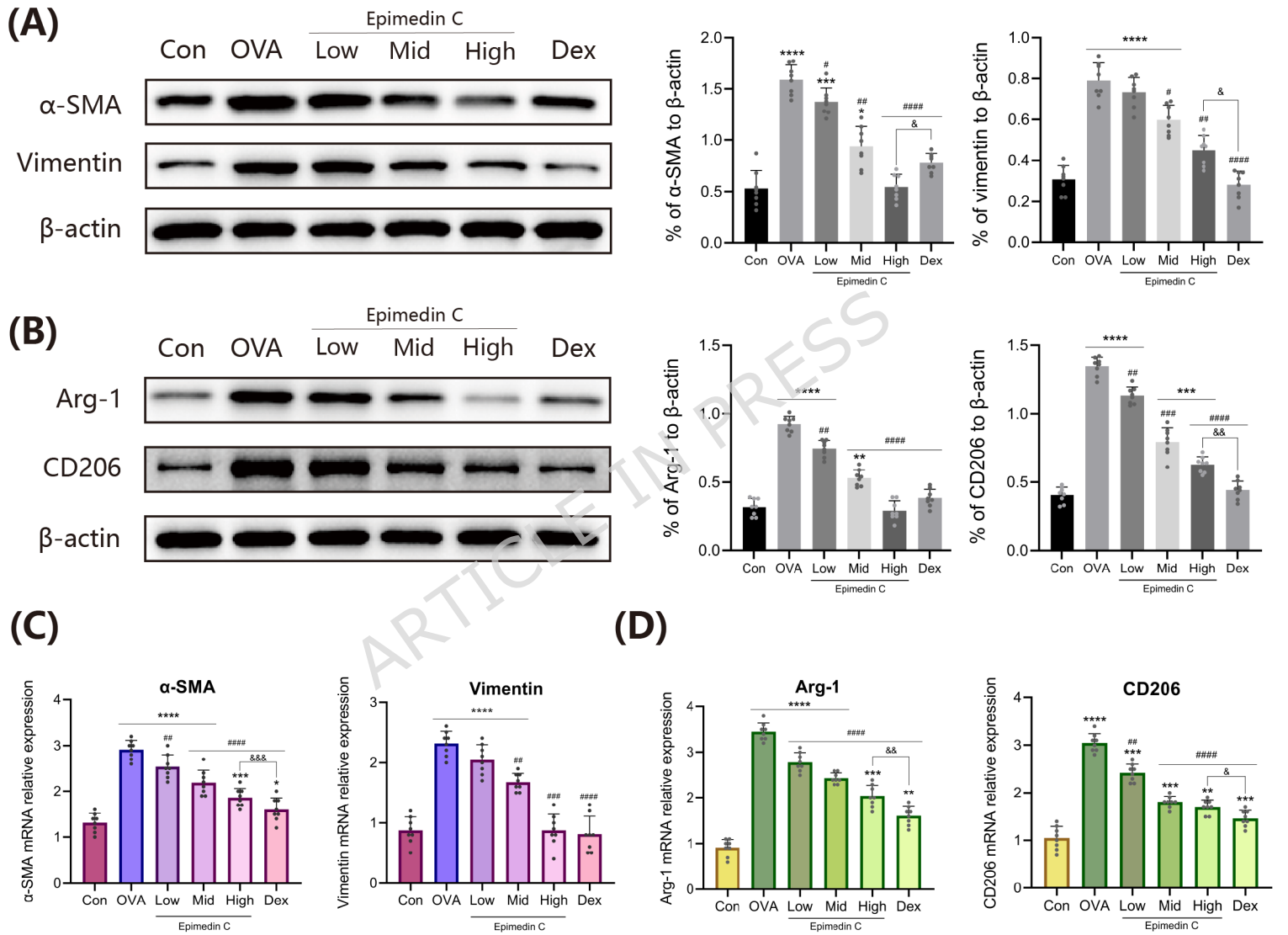


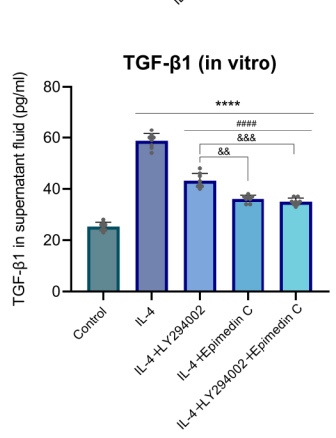
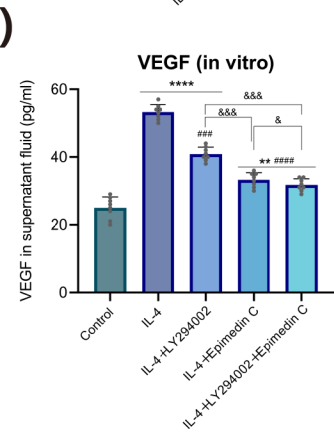
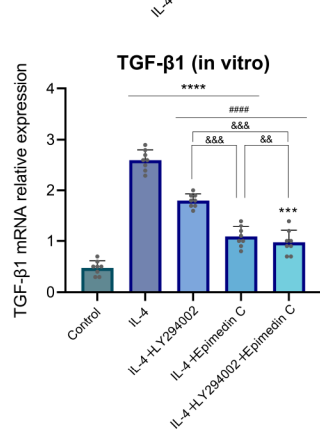
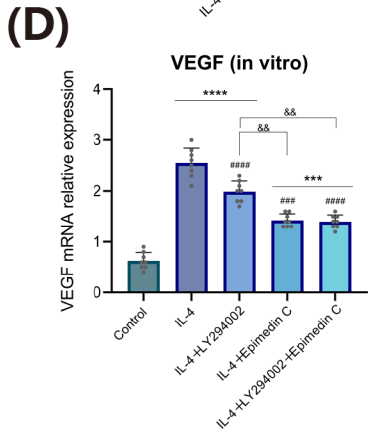
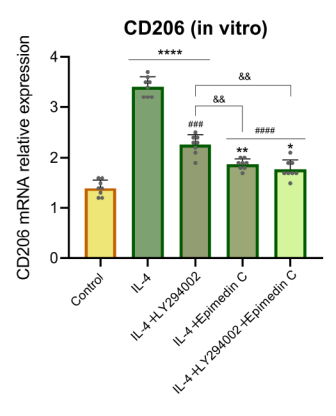
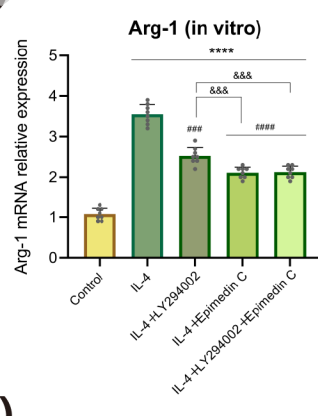
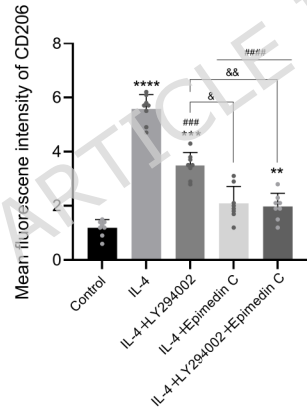
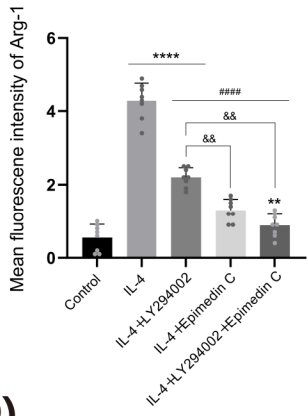
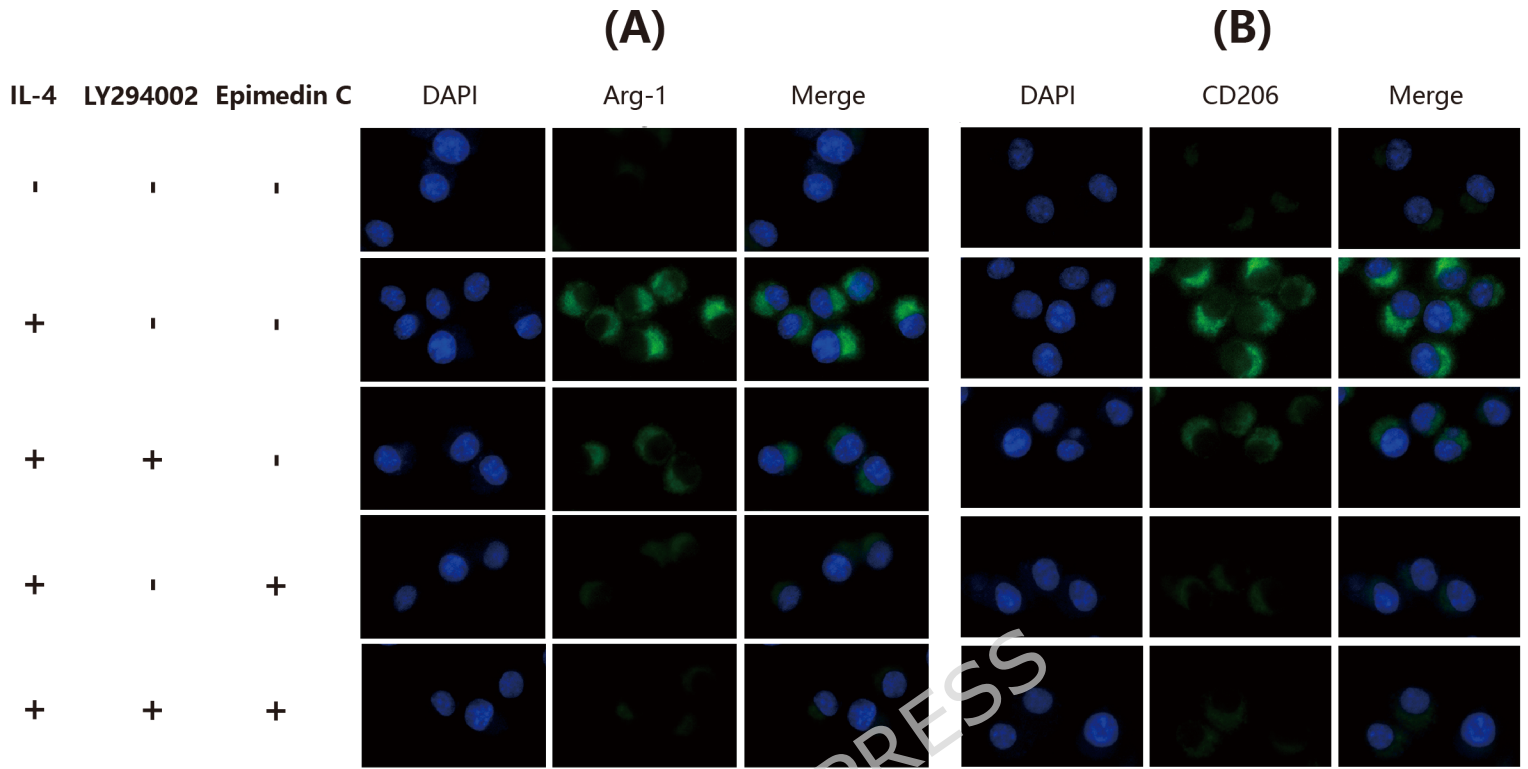
(C)

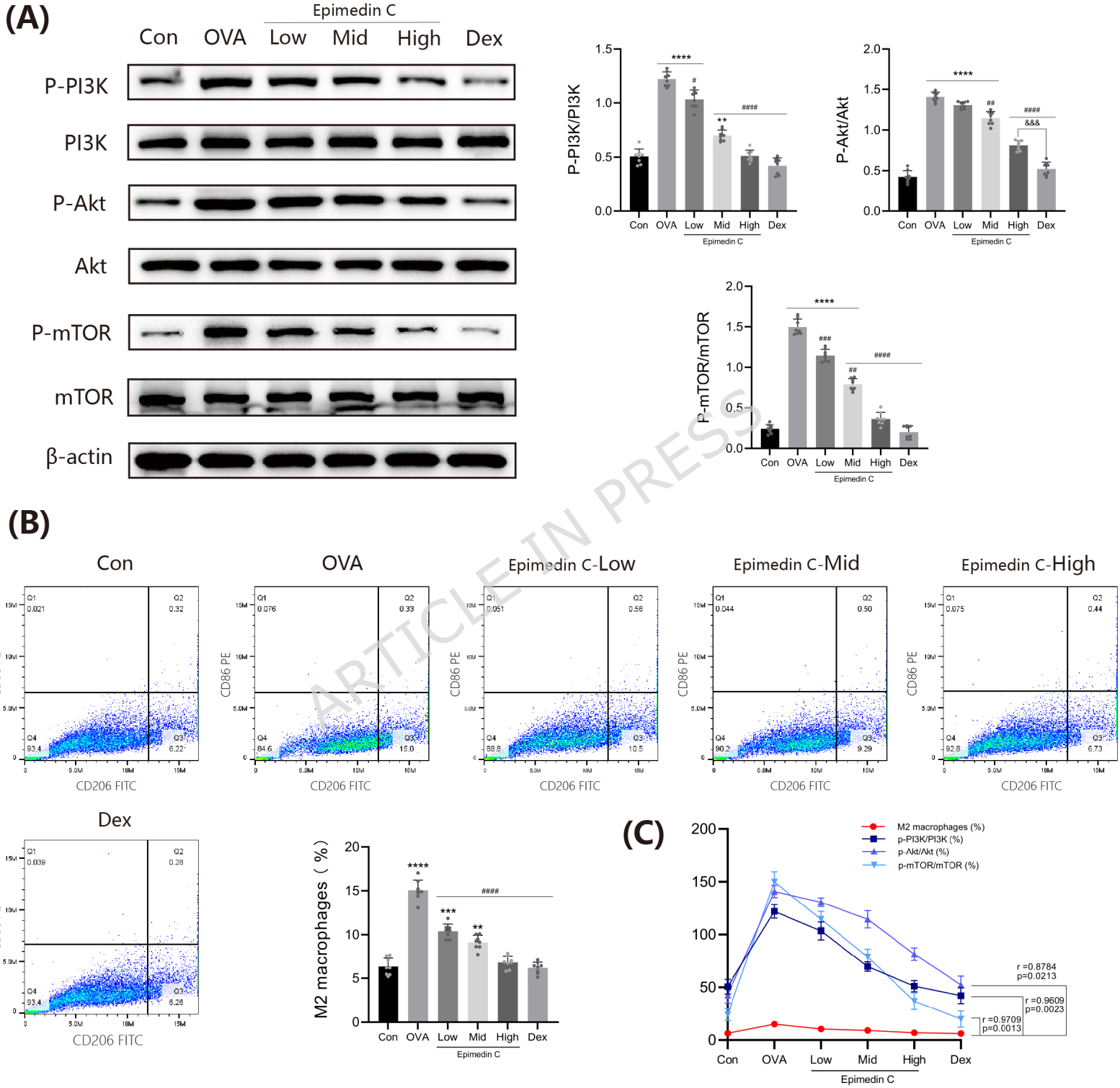


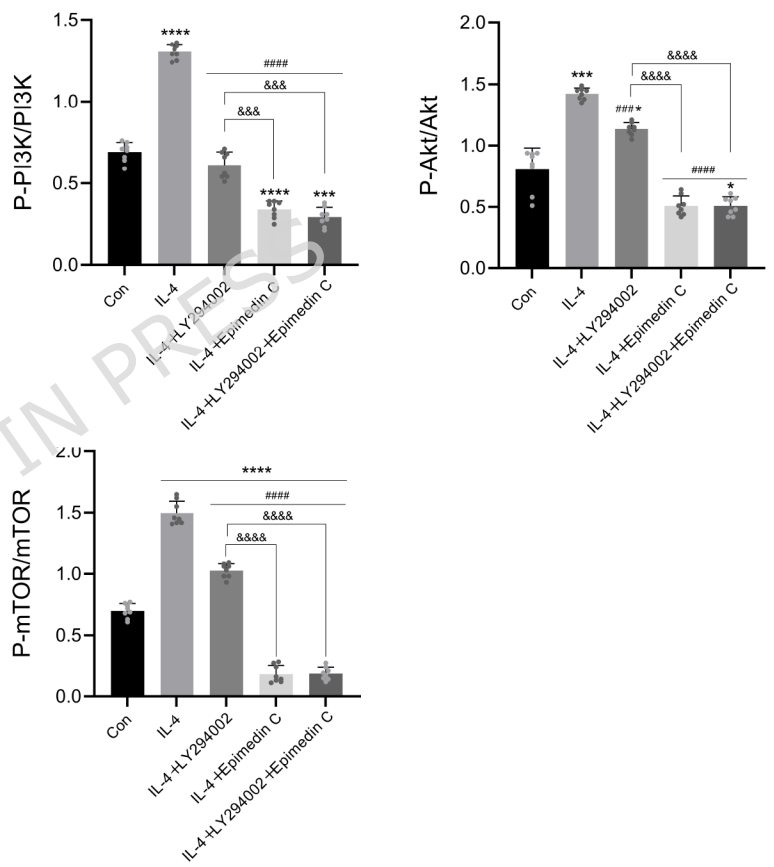
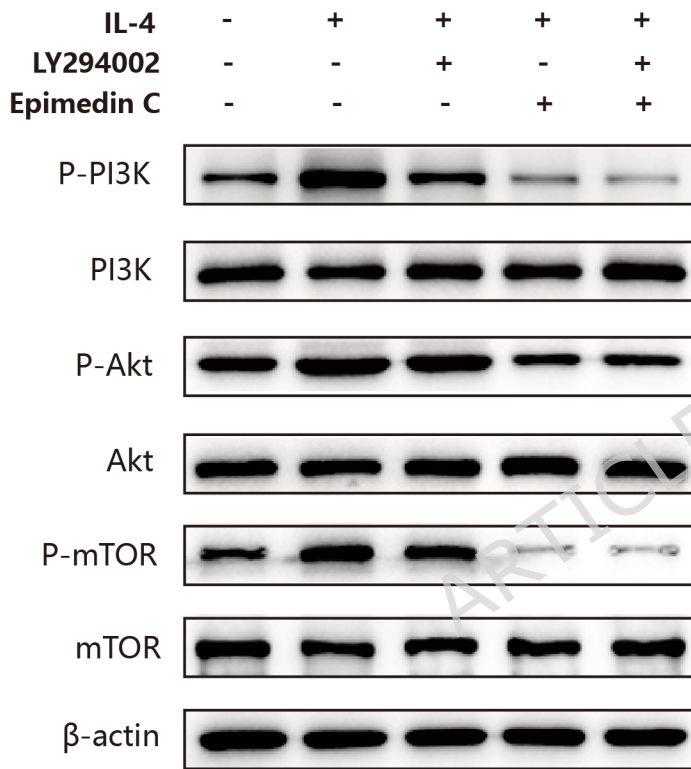
(D)

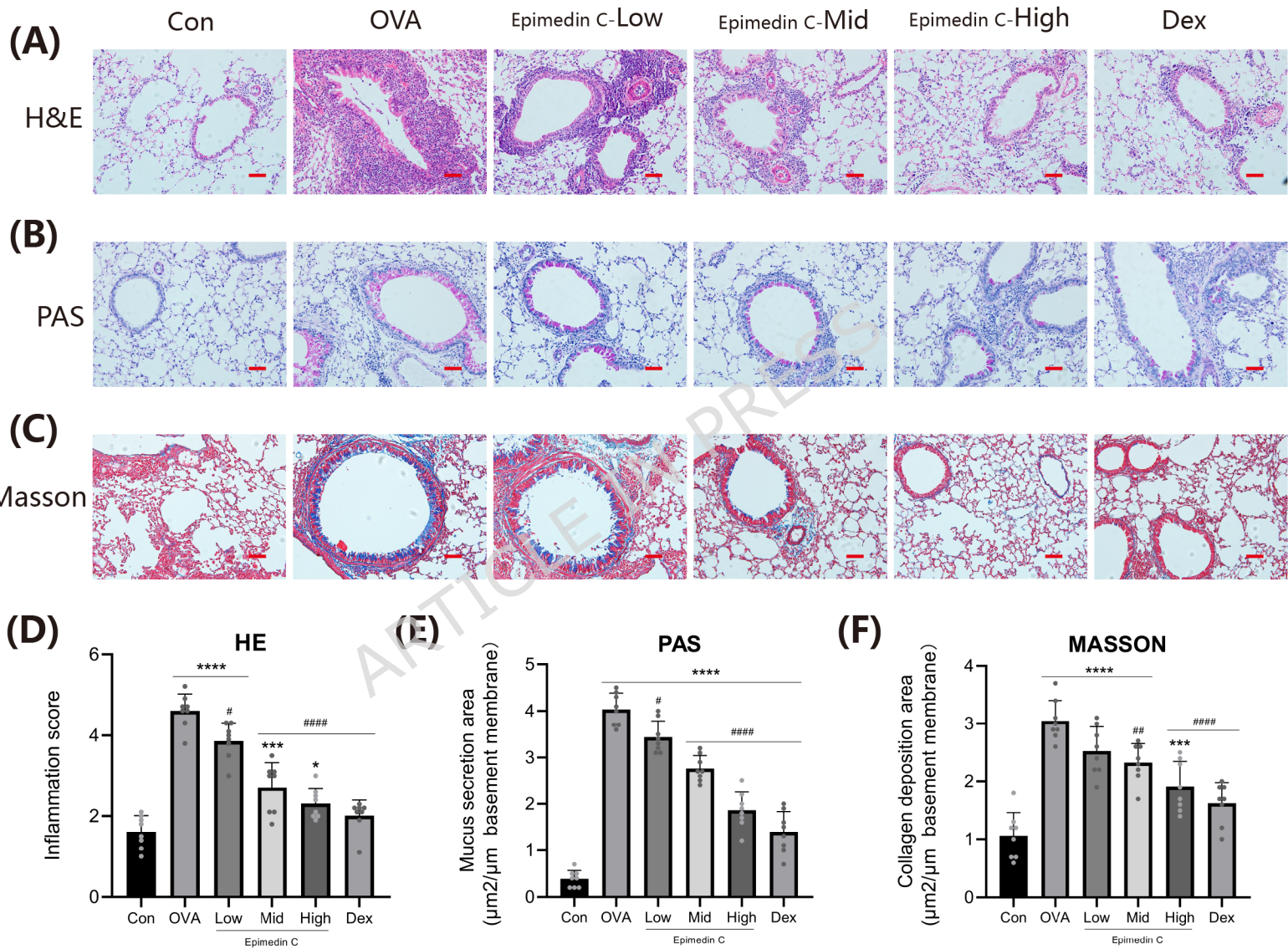




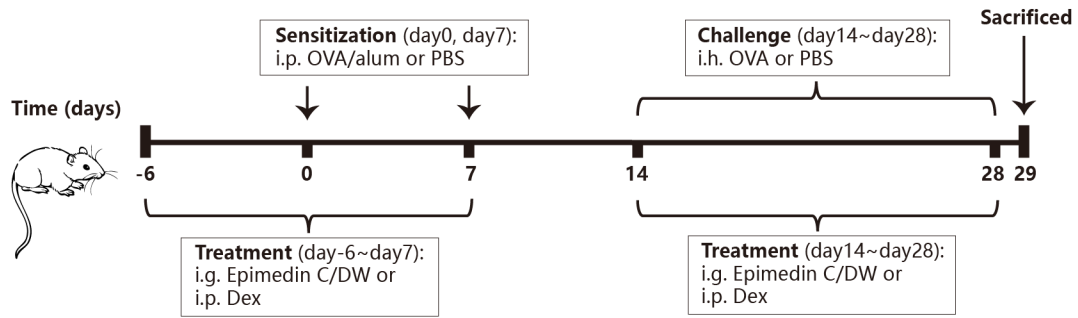




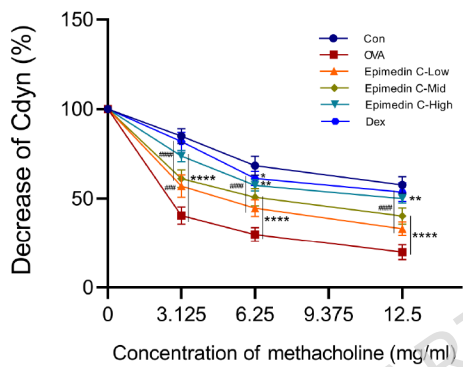
(A)



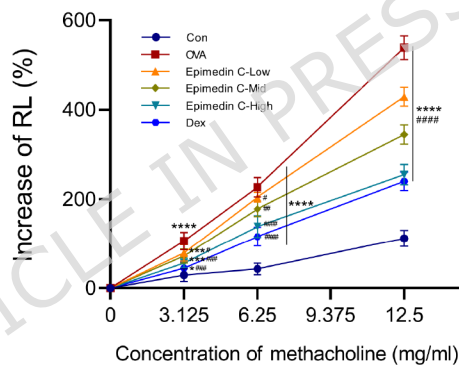
(A)



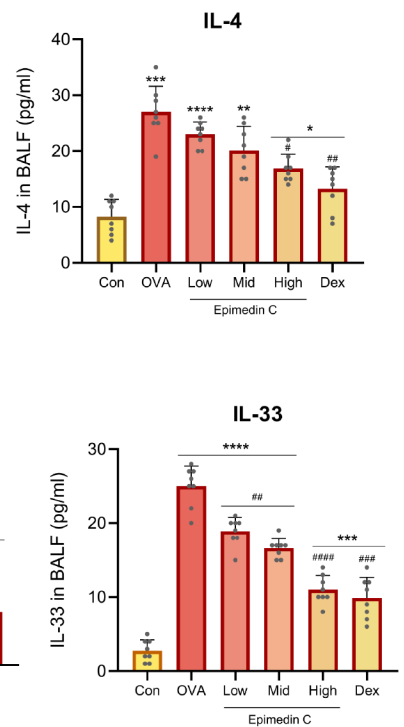
(B)

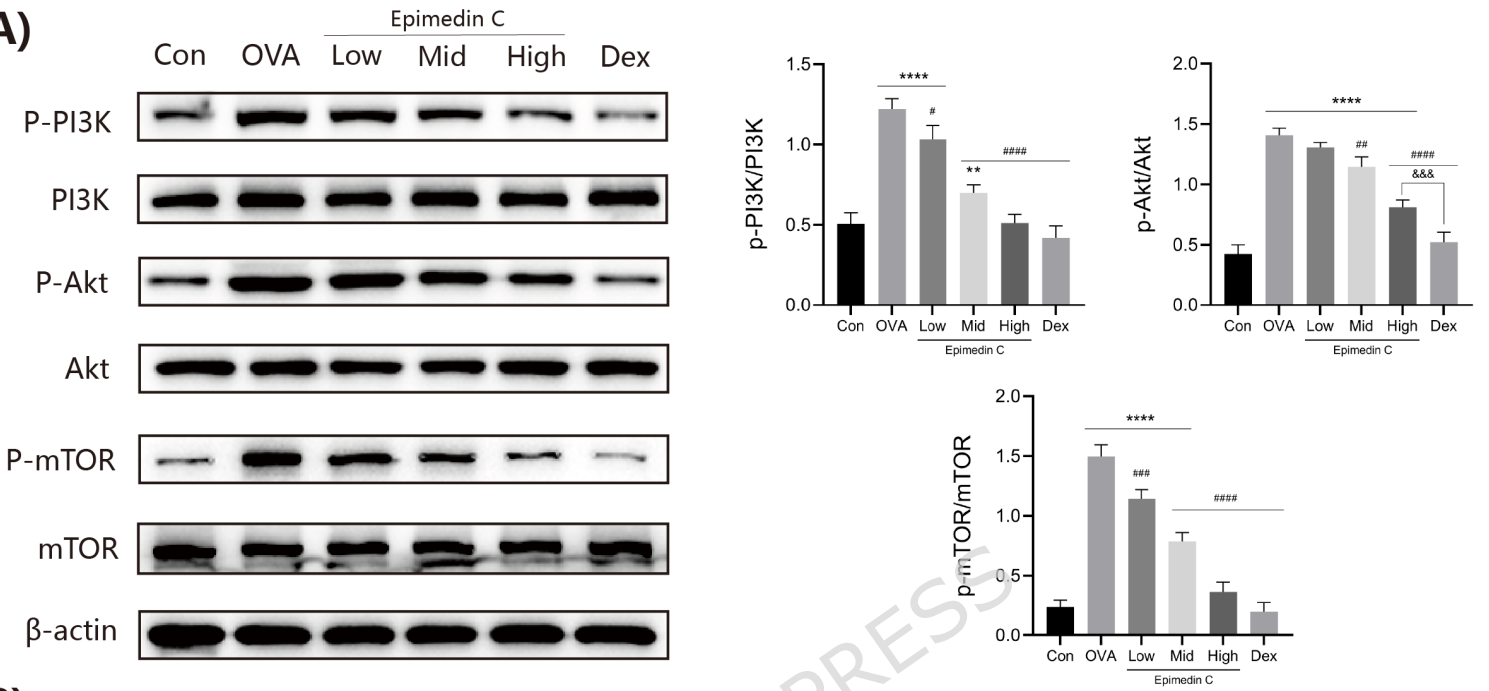
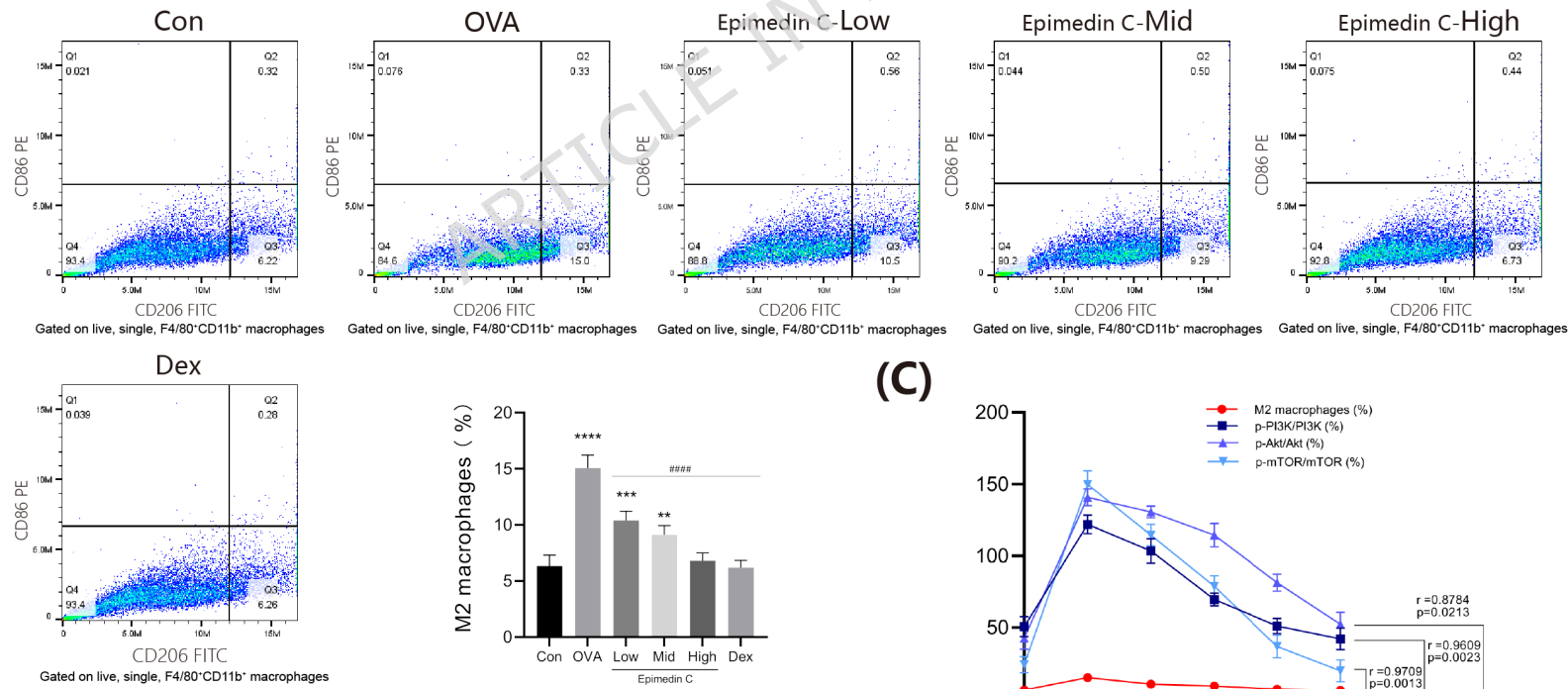
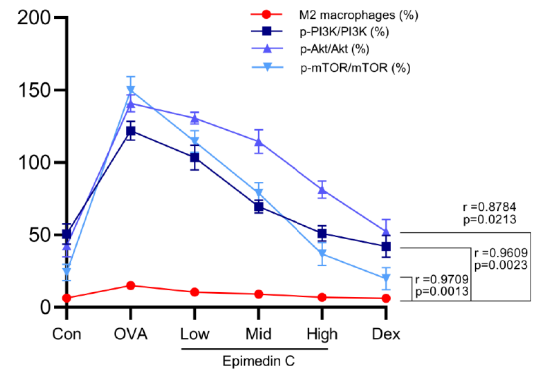


(C)



(D)



(A)**(B)****(C)**

(A)

